Acta Physiologica Sinica, April 25, 2004, 56(2): 137-146
http://www.actaps.com.cn

Research Paper

Temporal and spatial distribution of VIP, CGRP and their receptors in the development of airway hyperresponsiveness in the lungs

REN Yan-Hong, QIN Xiao-Qun*, GUAN Cha-Xiang, LUO Zi-Qiang, ZHANG Chang-Qing, SUN Xiu-Hong
Department of Physiology, *XiangYa Medical School*, *Central South University*, *Changsha 410078,China*

Abstract: To explore the role of intrapulmonary neuropeptides in the development of airway hyperresponsiveness, we established an animal model of airway hyperresponsiveness (AHR) in rabbits by using ozone exposure. With the model, after test of the mechanics of respiration and bronchoalveolar lavage assay, the levels of vasoactive intestinal peptide (VIP) and calcitonin gene-related peptide (CGRP) in the lungs were determined by radioimmunoassay, and the expression of mRNA coding receptors of these two neuropeptides was evaluated by reverse transcriptional-polymerase chain reaction (RT-PCR). At the same time, the distribution of VIP receptor-1 (VIPR1) and CGRP receptor-1 (CGRPR1) in lung tissues and its time-course were examined by *in situ* hybridization. The results showed: (1) in ozone-stressing groups, airway resistance increased significantly and typical inflammatory pathological changes were observed in pulmonary tissue slides, including neutrophil and eosinophil infiltration, mucus exudation and bronchial epithelial cells (BECs) shedding; (2) with elongation of ozone exposure, the levels of VIP and CGRP in the lungs increased at first, reaching a peak on d 2 to 4, then decreased slowly, and CGRP peaked somewhat earlier than VIP; (3) mRNA expression of the two neuropeptide receptors in the lungs changed in a similar manner like VIP and CGRP, but the high level of mRNA expression of VIPR1 lasted longer than that of CGRPR1; and (4) *in situ* hybridization for neuropeptide receptors demonstrated that, in unstressed control, VIPR1 and CGRPR1 positive cells appeared in the airway epithelium, pulmonary interstitial and focal areas of airway and vascular smooth muscles. With the elongation of ozone exposure, hybridization stained deeper and the majority of positive cells were located around the vessels and bronchus except a few in the alveoli. At 8 d, only a small number of positive cells were seen in the lungs. From the results, it is concluded that ozone-stressing can induce the development of AHR, in which VIP and CGRP may play important roles. That implies, through binding to CGRPR1, CGRP stimulates an early inflammation response which contributes in cleaning up of irritants, while VIP exerts a later dampening of pulmonary inflammation response. These two neuropeptides may play sequential and complementary roles in the development of AHR.

Key words: airway hyperresponsiveness; animal model; bronchial epithelial cells; neuropeptide

血管活性肠肽、降钙素基因相关肽及其受体在气道高反应动物肺内的时空分布

任雁宏, 秦晓群*, 管茶香, 罗自强, 张长青, 孙秀泓
中南大学湘雅医学院生理学教研室, 长沙 410078

摘 要: 为探讨内源性神经肽在气道高反应性形成中的作用, 我们以臭氧应激损伤动物气道上皮细胞, 建立气道高反应性动物模型, 并观察臭氧应激不同时间肺内血管活性肠肽(vasoactive intestinal peptide, VIP)、降钙素基因相关肽(calcitonin gene-related peptide, CGRP)含量变化以及 VIP 受体(VIPR1)、CGRP 受体(GRPR1) mRNA 在肺内表达、分布的改变。实验观察到, 臭氧应激组动物吸入乙酰甲胆碱后气道阻力高于正常对照组, 肺内呈现明显的炎症改变。随臭氧应激时间延长, 肺组织匀浆中 VIP、CGRP 浓度呈先增高后降低的双向改变, CGRP 达峰值时间早于 VIP。VIPR1、CGRPR1 mRNA 表达亦经历了双向过程, VIPR1 峰值持续时间长于 CGRPR1。在无应激对照组动物, 肺间质、支气管上皮细胞、血管内皮细胞、平滑肌细胞均有 VIPR1、CGRPR1 mRNA 表达。随应激时间的延长, 阳性细胞呈斑片状集中于气管、血管周围, 染色强度增加, 至臭氧应激第 8 天, 阳性染色细胞减少。因此我们推测, 臭

Received 2003-07-11 Accepted 2003-12-13

This work was supported by the National Natural Science Foundation of China (No. 30270586).

*Corresponding author. Tel: + 86-731-2650341. Fax: + 86-731-2650400; E-mail: xiaoqun1988@hotmail.com

氧应激可以诱导动物气道高反应性的形成。在炎症的早期, 以 CGRP 的作用为主, 与肺损伤早期炎症信号的传递有关, 以清除刺激原、及时终止致病原的作用; 炎症后期以保护机体、促进修复、减轻损伤为主, VIP 发挥主要作用。

关键词: 气道高反应; 动物模型; 支气管上皮细胞; 神经肽
中图分类号: Q472

Airway hyperresponsiveness (AHR), a characteristic feature of asthma, describes the tendency of bronchi to constrict excessively and respond aberrantly to various nonallergic and nonspecific challenge. Pathogenesis of AHR includes inflammation, thickening, hyperplasis and remodeling in the airway wall[1,2]. Several kinds of animal models were established, such as allergic asthma animal model[3] and occupational asthma animal model[4] in order to study the diseases characterized by AHR. These models have some similarities with human asthma[5]. At present, most of the studies on AHR are focused on allergic reaction but protective roles of airway epithelium is ignored. The airway epithelium is a physical barrier that protects sensory nerves and smooth muscle from being directly stimulated by inhaled irritants[6]. In addition, epithelial cells release mediators, which can adjust airway microenvironment. Recent studies in our laboratory have shown that ozone exposure can exert stressful action on airway epithelial cells and increase nitric oxide release[7]. In order to prove the hypothesis that dysfunction of airway epithelium is the initial step in the development of AHR in the present study, using ozone-inspiration to damage the airway epithelium of rabbits, we created a novel type of animal model of AHR and a method to measure the airway resistance realtimely *in vivo* respiration.

Neuropeptides such as vasoactive intestinal peptide (VIP) and calcitonin gene-related peptide (CGRP) are found in high level in the pulmonary tissue[8,9]. When an irritation acts on the local tissue, they are released from the sensory nerves and APUD (amine precursor uptake and decarboxylation) cells in the lungs[9]. Previous studies in our laboratory showed that VIP attenuated cell damage caused by oxidant challenge[10], inhibited inflammatory mediators release[11] and adhesion of leukocytes to airway epithelial cells [12]; however, CGRP showed effects contrary to VIP, for instance, promoting the release of interleukins and the adhesion of leukocytes to airway epithelial cells[11,12]. These studies suggest that VIP and CGRP may play important roles in the pathogenesis of several airway diseases such as asthma and mediate effects that contribute to asthmatic airway dysfunction through binding to their receptors present in the airways. However, there is no direct evidence identifying that VIP or CGRP are involved in the development of AHR. Therefore, to explore the role of VIP and CGRP in the development of AHR, the purpose of the present study was to detect the changes in VIP and CGRP levels, mRNA expression of VIPR1 and CGRPR1, and the distribution of VIPR1 and CGRPR1 in the lungs.

1 METHODS AND MATERIALS

1.1 *Animals and materials*. New Zealand white rabbits were supplied by the Experimental Animal Center, XiangYa Medical College, Central South University; RM6240-C biology signal collection system was purchased from Chengdu Instrument Factory (Chengdu), small animal respirator from Tely Anesthesia and Respiration Instrument Company (Nanchang). Interleukin -1 (IL-1) radioimmunoassay kit and CGRP radioimmunoassay kit were purchased from Dongya Immune Research Institute (Beijing), VIP radioimmunoassay kit was from Hikery Immune Research Institute (Beijing). Ozone generator was supplied by No-ferrous Metal Research Institute (Changsha). Methacholine, DEPC, TRIZOL reagent were purchased from Sigma. Reverse transcriptase kit (Promega), *in situ* hybridization kit and primers synthesis were provided by Boster Biological Technology Co., Ltd. (Wuhan).

1.2 *Experiment groups*. The study consisted of two parts. In part 1, an animal model with AHR was set up and used for measurement of respiratory mechanics and assay of bronchoalveolar lavage fluid. Twelve New Zealand white rabbits were randomly divided into two groups: (1) six rabbits in the control group breathed only filtered room air; and (2) six in the ozone-stressing group inhaled 2.0 ppm of ozone 1 h/d for three days, while they were awake and breathing spontaneously in a chamber (25 cm×25 cm×40 cm). Part 2 composed of four experimental groups and one control group, for evaluating the possible involvement of endogenous VIP and CGRP in the development of AHR. Five animals in each experimental group were exposed to 2.0 ppm ozone 1 h/d for 1, 2, 4 and 8 d, respectively. In control group, 5 animals were caged on the same condition but breathed only filtered room air. In part 2, the changes in VIP and CGRP levels, the mRNA expression of VIPR-1 and CGRPR-1, and the distribution of the mRNAs of VIPR1 and CGRPR1 in lung tissue were investigated at

different ozone-stressing time points.

1.3 *Measurement of lung mechanics*. The animals were challenged by inhaling aerosolized methacholine (4 mg/ml) at 12 h after the last ozone exposure. After challenge, all animals were anesthetized with 25% ethyl carbamate (4 ml/kg) and laid supine in comfortable position on a small mold, then intubated with a 6 mm tracheal cannula. A polyethylene catheter (2.0 mm o.d., 1.0 mm i.d.) with some poles at the end of the catheter was passed into the tracheal cannula and kept at a certain distance (approximately 11 ± 0.5 cm) from 5~6 cricoid during experiment. The space between tracheal cannula and the catheter was sealed. The other end of the catheter was connected to a pressure transducer and the collateral arm of tracheal cannula to an airflow transducer respectively, so that intrapulmonary pressure and airflow signals could be recorded synchronically. Airway resistance (AR) then could be calculated according to the formula: AR= (intrapulmonary pressure-atmospheric pressure)/airflow.

1.4 *Bronchoalveolar lavage (BAL)*. After the detection of airway resistance, rabbits were killed by bleeding from femoral artery and subjected to bronchoalveolar lavage. This procedure was performed as follows: 15 ml of sterilized saline solution (37ºC) was introduced through the tracheal tube and gently recovered 1 min later. The lavage was repeated and the recovered fluid was mixed. Volumes of total BAL fluid were 25 ± 1 ml per rabbit. Then the recovered fluid was immediately centrifuged for 10 min at 1500 ×g, 4ºC. The supernatants were stored at −70ºC for chemical assay later. The pellet was washed with Tris-buffered ammonium chloride solution (pH 7.2) to lyse the contaminated red blood cells, then centrifuged again. The pellet was re-suspended with saline solution and the total number of cells was counted under light microscope. The viability of the cells was confirmed more than 80% by typan blue exclusion technique. Smears were stained with Giemsa to classify different cell types.

1.5 *Protein and IL-1 analyses in bronchoalveolar lavage fluid* (*BALF*). Total protein concentration was determined in each sample by the Lowry method. Radioimmunoassay of IL-1 was performed according to the protocol. Briefly, ^{125}I-IL-1beta was added to BAL samples or standard reactants that were incubated at 4ºC overnight. Then IL-1 beta antiserum was added and incubated for 20 min at room temperature. After another centrifugation at 4ºC at 3500 × g for 25 min, the supernatants were discarded and radio-intensity of ^{125}I in the pellets was measured using γ-counter, and the concentration of IL-1 was calculated according to the curve of standard reaction.

1.6 *Histopathologic examination of lung injury and inflammation*. To examine injury and inflammation in the lungs, rabbits were killed as described above and the lungs with trachea were removed and fixed in 10% formaldehyde immediately. After tissue fixation, specimens of trachea and lung lobes were embedded in paraffin wax, then 5 μm thick sections were made and stained with hematoxylin-epsin, and checked under light microscope.

1.7 *Determination of VIP and CGRP levels in lung tissue homogenates*. An intrathoracic airway specimen, including the lower trachea and extrapulmonary bronchi, was removed from each animal immediately after anesthesia. The specimen was weighed, boiled (95ºC) for 10 min in 1 mol/L acetic acid, then neutralized with 1 mol/L NaOH and homogenized. The homogenates were transferred into a polypropylene tube and centrifuged (3000 × g, 4ºC, 20 min). Supernatant fractions were removed for radioimmunoassay of VIP and CGRP. For measurement of CGRP, 200 μl of supernatant was incubated at 4ºC for 48 h with 100 μl of anti-CGRP antibody which cross-reacts with both CGRP I and CGRP II. Standard curves were established with synthetic CGRP, ranging from 20 to 1200 pg/tubes, then 100 μl of ^{125}I-CGRP was added into each tube and incubated for an additional 24 h at 4ºC. Finally, 500 μl of separating medium was added and centrifuged (3500 × g, 4ºC) for 20 min. The supernatant fractions were decanted , and the radioactivity in the remaining pellet was tested. The level of VIP-like immunoreactivity (VIP-LI) was measured in a manner similar to that for CGRP-LI described above.

1.8 *Total RNA extraction and semi-quantitative RT-PCR*. Total RNA was isolated from 30 mg of the tissue at the peripheral region of the lungs by using an RNasy Minikit (QIAGEN, Valencia, CA). Total RNA was reversely transcribed and amplified by a two-step RT-PCR. Appropriate upstream and downstream primers were designed according to the cDNA sequence of human Genebank. For VIPR-1 gene (GI:6981703), the sense primer is 5'AGC AGT GCC TGG AGG AGG 3' (start at 201 bp downstream of coding start site), and the antisense primer is 5'GAA GAG ATG CAT GTG GAT GTA GTT 3' (end at 606 bp downstream of coding start site), the expectant length of the product is 406 bp. For CGRPR-1 gene (GI:1321593), the sense primer is 5'TTTACTGCAACAGAACCTGGAT 3' (start at 742 bp downstream of coding start site), and the antisense primer is 5'GAAATCCCCAGCCAAGAAAAT 3' (end at 1341 bp downstream of coding start site), the ex-

pectant length of the product is 600 bp. Because the sequence data of rabbit was not available at the time this study was undertaken, we compared the sequence in human , rat and mouse, and chose a high conserved and homogenous segment to design the primers. Furthermore, we checked specificity of PCR products by Southern blot with a specific probe (the data are not showed in this paper). To normalize the data of VIPR-1 or CGRPR-1 mRNA expression, G3PDH (GI: 406106, 723~1011 bp) was selected as internal control, the primers are 5'AAG GTC ATC CCC GAG CTG AAC 3' and 5'CAT ACC AGG AAA TGA GCT TCA 3' and the expected length of the product is 289 bp. Conditions for PCR were: after a "hot-start" at 95ºC for 3 min prior to the addition of Taq DNA polymerase, 35 cycles of amplification were performed at 94ºC for 30 s, 62ºC for 20 s, 72ºC for 50 s (CGRPR1), and at 94ºC for 30 s, 63ºC for 20 s, 72ºC for 50 s (VIPR1), then kept at 72ºC for 10 min. The PCR products were checked by electrophoresis in a 2% agarose gel. The intensity of each band, visualized by ethidium bromide staining , was quantified by gray analysis of bands.

1.9 In situ *hybridization*. Tissues were fixed in 4% paraformaldehyde in DEPC-treated PBS for 2 h at room temperature before routine processing , washed in PBS (at room temperature), dehydrated in an ethanol dilution series and infiltrated with xylene. The tissue was embedded, sectioned (8~10 μm thick), and baked onto Lys-coated slides (at 42ºC for 1~2 d). *In situ* hybridization was carried out according to the method of the manufacturer with some modifications. Briefly, the tissues were rehydrated, at the same time treated with proteinase K for 5 min at 37°C. Sections were prehybridized in 20 μl of hybribuffer for 3 h at 38°C and then incubated in a humidity chamber without coverslips for 15 h at 42°C with 20 μl of hybribuffer containing digoxin-labelled probe. Following hybridization, slides were washed in DEPC-treated 2 × SSC (37ºC) once for 5 min, 0.5 × SSC (37°C, twice for 15 min each) and then 0.2 × SSC (37°C, once for 15 min), incubated with mouse anti-digoxin at 20~37°C for 30 min and washed with 0.5 mol/L PBS three times, each for 5 min. The slides were then incubated with anti-mouse biotin IgG at 20~37°C for 20 min, washed with 0.5 mol/L PBS three times, each for 5 min, and again incubated with SABC at 20~37°C for 20 min, washed with 0.5 mol/L PBS four times, each for 5 min. The color reaction was developed with the addition of DAB and sealed with xylene.

1.10 *Statistic analysis*. Unless otherwise stated, data are reported as mean±SEM. A Student's *t* test was used for the comparison of two groups. When data were not normally distributed, a rank sum test was carried out. One-way analysis of variance (ANOVA) on ranks according to a Kruskal-Wallis rank sum test was performed. A significant difference was assumed to exist when $P<0.05$.

2 RESULTS

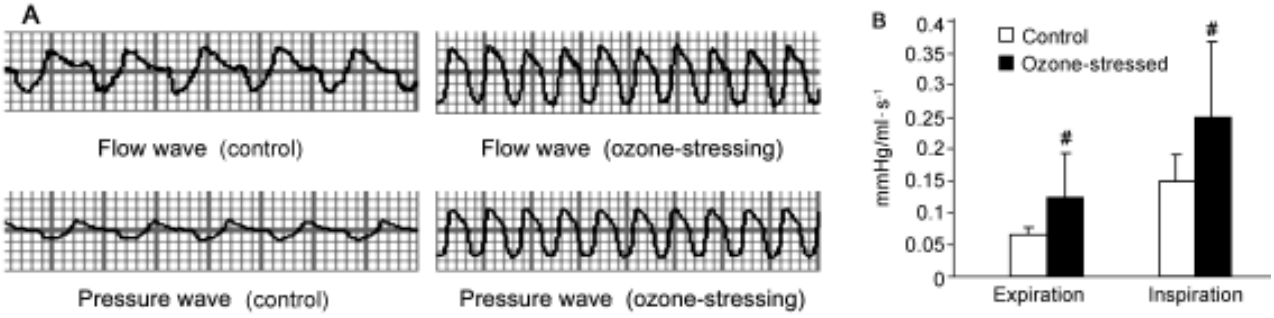

Fig. 1. *A*: Dynamic records of intrapulmonary pressure and air flow. *B*: Effect of ozone on airway resistance. $n=6$, $^{\#}P<0.05$ *vs* control.

Table.1. Bronchoalveolar Lavage Fluid analysis

Group	Cell counts ($\times 10^5$)					IL-1	Total protein
	Total cells	Lymphocytes	Neutrophils	Eosinophils	Macrophages	(ng/ml)	(μg/μl)
Control	1.40 ± 0.02	0.14 ± 0.03	0.06 ± 0.03	0.005 ± 0.0003	1.20 ± 0.02	1.167	0.529
Ozone	4.40 ± 0.09$^{\#\#}$	0.87 ± 0.18$^{\#\#}$	0.43 ± 0.09$^{\#\#}$	0.05 ± 0.03$^{\#\#}$	3.00 ± 0.22$^{\#\#}$	1.448*	2.203$^{\#\#}$

$n=6$, $^{\#\#}P<0.01$ $^{*}P<0.05$.

2.1 Pulmonary function

There is a significant difference in airway resistance between control and ozone exposure groups. Methacholine challenge evoked a rapid and intense increase in airway resistance in both expiration and inspiration (Fig. 1*A, B*).

2.2 Bronchoalveolar lavage analysis

The experimental group exposed to ozone showed a significant increase in total cell numbers compared with the control group, especially the number of macrophages, neutrophils and eosinophils increased obviously. The concentration of total protein and IL-1 in BALF also increased in the ozone stress group. These data indicate that an inflammatory response in the lung was induced by ozone exposure (Table1).

2.3 Histopathologic examination

Typical pathological inflammation changes in the lung were observed in ozone exposure group, including airway constriction, airway epithelial cell shedding, inflammatory cell infiltration in airway lumen, alveoli and pulmonary interstitial. However, these pathological changes were not seen in the control animals (Fig. 2).

2.4 Variation of VIP and CGRP levels in the lungs

In ozone exposure groups, the concentrations of VIP and CGRP in the lungs began to rise within 48 h and peaked at 4 d (VIP) and 2 d (CGRP), respectively, then decreased

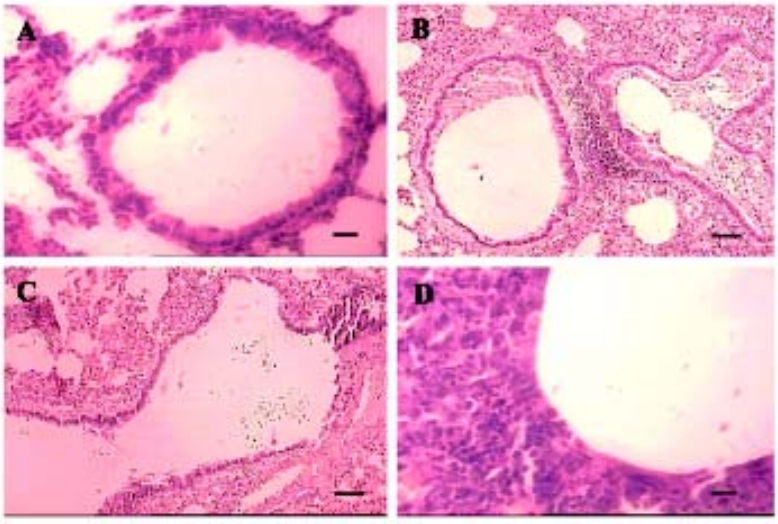

Fig. 2. Histopathology of lung injury model induced by ozone exposure. *A*: Control: no bronchoconstriction and inflammatory cells infiltration in bronchi. HE-staining. Scale bar, 10 μm. *B*: Ozone-stressing: inflammatory cells infiltration and mucus exudation in bronchi. HE-staining. Scale bar, 50 μm. *C*: Ozone-stress: BECs in bronchi shedding. HE-staining. Scale bar, 50 μm. *D*: Ozone-stressing: inflammatory cells infiltration in pulmonary interstitial. HE-staining. Scale bar, 10 μm.

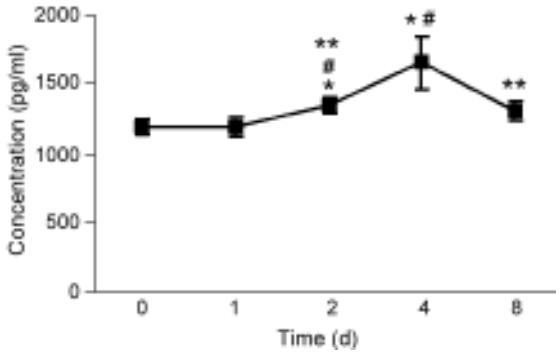

Fig. 3. Concentration of VIP in the lungs rose at first and peaked on d 4, then decreased slowly. n=5, $^{*}P$<0.05 *vs* d 0, $^{\#}P$<0.05 *vs* d 1, $^{**}P$<0.01 *vs* d 4.

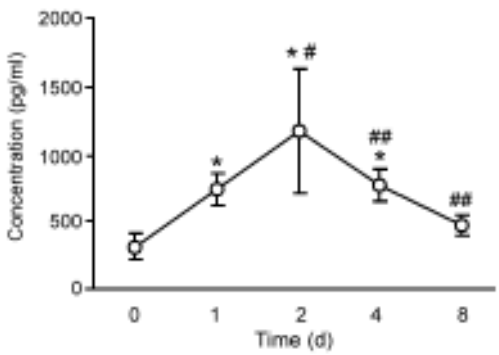

Fig. 4. Concentration of CGRP in the lungs rose and peaked on d 2, then decreased slowly. n=5, $^{*}P$<0.01 *vs* d 0, $^{\#}P$<0.01 *vs* d 1, $^{\#\#}P$<0.05 *vs* d 2.

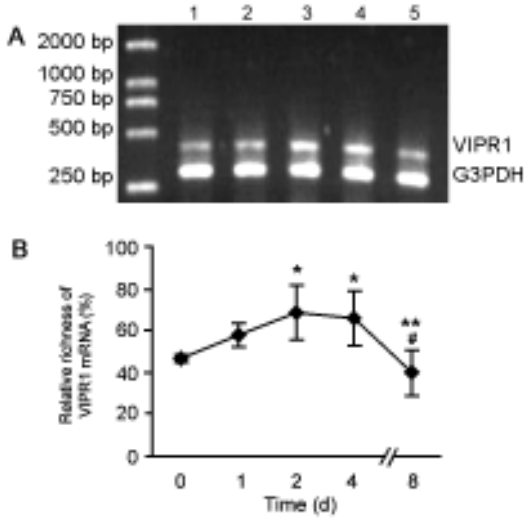

Fig. 5. *A*: RT-PCR shows the mRNA expression of VIPR1 at various ozone-stressing time points. Lanes 1 to 5 are on d 0, 1, 2, 4, and 8. *B*: mRNA expression of VIPR1 in lung at various ozone-stressing time points. n=4. $^{*}P$<0.05 *vs* d 0, $^{\#}P$<0.05 *vs* d 4. $^{**}P$<0.05 *vs* d 2.

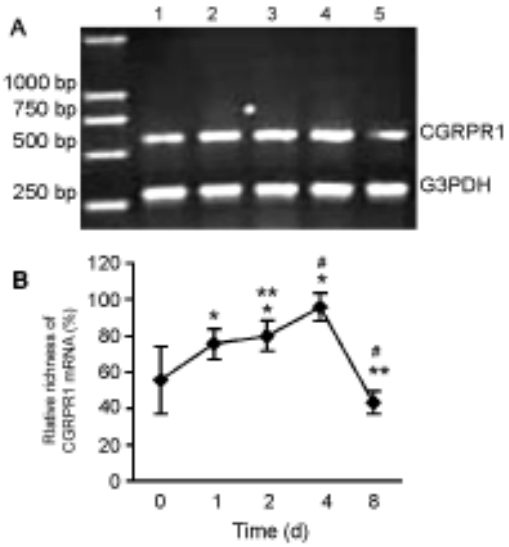

Fig. 6. *A*: RT-PCR shows the mRNA expression of CGRPR1 at various ozone-stressing time points. Lanes 1 to 5 are on d 0, 1, 2, 4, and 8. *B*: mRNA expression of CGRPR1 in lung at various ozone-stressing time points. n=4, $^{*}P$<0.05 *vs* d 0, $^{\#}P$<0.05 *vs* d 1, $^{**}P$<0.05 *vs* d 4.

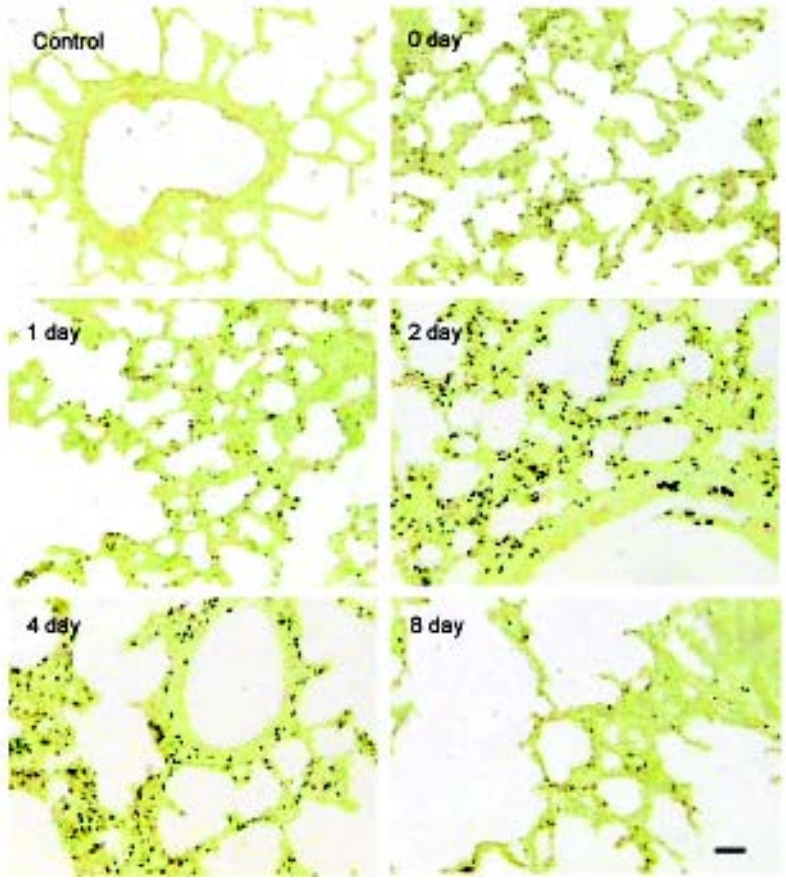

Fig. 7. Hybridization *in situ* shows the distribution of VIPR1 mRNA in the lung at various ozone-stressing time points. Scale bar, 50 μm.

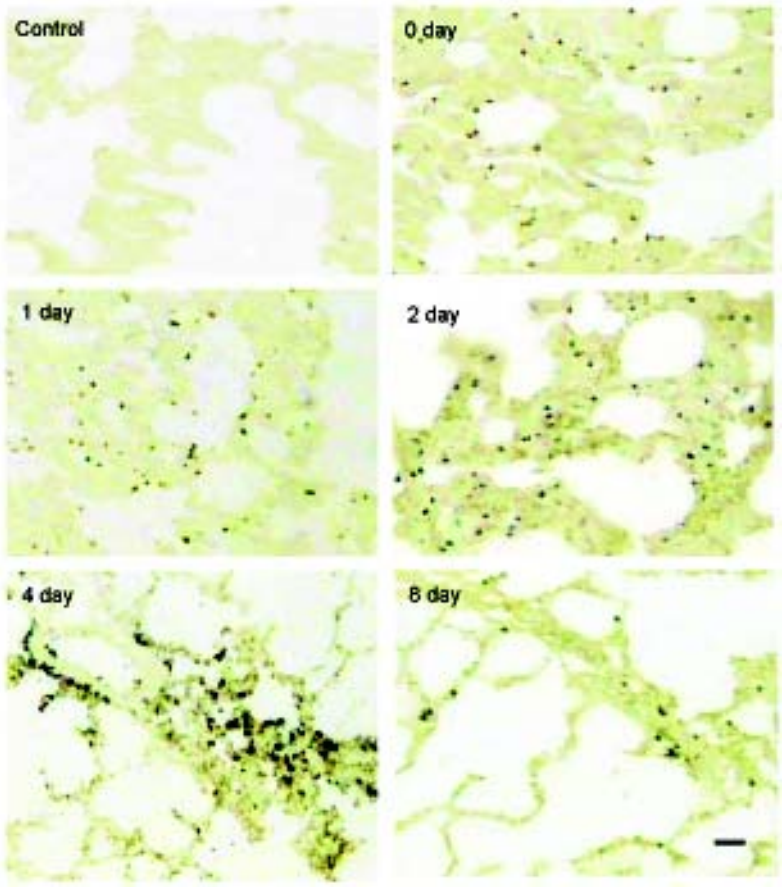

Fig. 8. Hybridization *in situ* shows the distribution of CGRPR 1 mRNA in the lung at various ozone-stressing time points. Scale bar, 50 μm.

gradually to the baseline (Figs. 3 and 4). The time course of VIP and CGRP levels were insistent with that of pulmonary pathological changes.

2.5 mRNA expression of VIPR-1 and CGRPR-1 in the lungs

Using a gel image analysis system, mRNA was quantified by measuring the gray of the cDNA bands obtained by RT-PCR that encodes each type of receptor. The level of gray for each receptor cDNA was then normalized with the gray of corresponding G3PDH cDNA band which was concurrently amplified. That is, the ratio of gray density of each target product band to the gray density of its correspond G3PDH product band was calculated, so that a relative value of original copy number of target gene mRNA could be estimated. A time-dependent increase in the mRNA expression of these two receptors has been observed during ozone exposure. The amounts of mRNA encoding VIPR1 increased from baseline to maximal level within 2~4 d and decreased to baseline nearly at 8 d. (Fig. 5*A,B*). The expression of mRNA encoding CGRPR1 changed in a similar manner to those observed in VIPR1 mRNA (Fig. 6*A*, *B*).

2.6 *In situ* hybridization analysis of neuropeptide receptors in lung tissue

The results in our experiments showed that, on d 0, VIPR1 were expressed in airway epithelium, pulmonary interstitial, focal areas of airway and vascular smooth muscle. At 1 d, the distribution of VIPR1-positive cells has no significant change. Within 2 to 4 d, hybridization staining deepened and the majority of VIPR1-positive cells were located around vessels and bronchus, with a few in alveolar; however, at 8 d, few positive cells were seen in lung (Fig. 7).

At d 0, CGRPR1 mRNA hybridization signal was detected mainly in pulmonary interstitial and a little in smooth muscle cells. At 2 d, hybridization staining deepened and the majority of CGRPR1-positive cells were also located around vessels and small bronchus. Up to d 8, only diffuse weak CGRPR1 mRNA signals were detected in the lung (Fig. 8).

3 DISCUSSION

The airway is lined with epithelial cells which form a barrier between inhaled substance and the inner components of the airway. It has become increasingly clear that epithelial cells with active secretion and metabolism function not only serve as a structural support and anatomic barrier but also are sources of many inflammatory mediators. Bronchial epithelial cells (BEC) can exchange information with the tissues and cells nearby, regulating functions of these tissues. In turn BECs also adjust functions or metabolism of themselves so as to adapt to the changes in chemical signals in local microenvironment[6,13]. Based on this new conception, the present study tried to set up a novel animal model through stressing bronchial epithelial cells with ozone exposure and explored the pathogenesis of AHR. Airway resistance is a very important parameter to measure airway responsiveness to irritants. During the process of experiments, we measured airway resistance by way of recording intrapulmonary pressure and airflow synchronically in real time, which is more creditable and direct than those indirect criteria indexes such as respiratory frequency, respiratory depth and behavior of animals. Our results have shown that, after challenge at the same condition, animals in ozone-stressing group have an increased airway resistance compared with controls, which is co-insistent with histopathologic examination and bronchoalveolar lavage analysis. These data suggest that imbalance of homeostasis in airway microenvironment or damage of BECs may be the initial step in the development of AHR.

A large body of evidence supports the role of the peptidergic nervous system in mediating inflammation of conducting airways[8,14,15]. Airways are richly innervated with sensory nerve fibers. Non-adrenergic non-chollinergic (NANC) nerves are the third nervous system besides adrenergic and cholinergic nerves. There is increasing evidence that the main transmitters of NANC inhibitory (NANC-I) and NANC excitatory (NANV-e) nerves are vasoactive intestinal peptides (VIP) and sensory neuropeptides (SNPs), respectively[16,17].

Vasoactive intestinal polypeptide (VIP), a 28-amino acid neuropeptide, is one of the most abundant, biologically active peptides found in the human lung[8]. VIP-immunoreactive nerve fibers are present in the tracheobronchial airway smooth muscle layer, the walls of pulmonary and bronchial vessels and around submucosal glands[18,19]. VIP influences many aspects of pulmonary biology in human airways by binding with VIP receptors. Several studies using receptor binding techniques have been performed to demonstrate the presence of VIP receptors and have shown abundant binding in different parts of the lungs[20]. Two types of VIP receptors have been cloned and characterized in the past years,VPAC1 and VPAC2 respectively. Because there is a high expression of VPAC1 in the lungs, this study examined the concentration of VIP, the mRNA expression and distribution of VPAC1 at a series of ozone-stressing time points. VIP is a dilator for systemic and pulmonary vessels, a powerful stimulant for chloride ion transport across airway epithelium, a potent stimulant of mucus secretion, and may also act as an anti-inflammatory mediator in airways[21]. It has been shown that VIP has antioxidant activity, enabling it to protect lung from injury that will occur during inflammation or asthma[22,23]. Our results from the experiments showed that the concentration of VIP in lung increased within 48 h and peaked at 4 d, and then decreased gradually, which is in accordance with other studies[24]. Since the magnitude of pulmonary inflammatory response is ozone-stressing time dependent, these data indicate a correlation between neuropeptide concentration in lung and the intensity of inflammatory response. In earlier period of lung injury, VIP in lung had a compensatory increase, which is benefit to ease lung injury. With aggravation of lung injury, VIP-immunoreactive nerve fibers decreased and inflammatory cells released various hydrolytic enzymes such as trypure and chymetin[25], which make VIP degrade.

Calcitonin gene-related peptide (CGRP) is a 37-amino acid neuropeptide generated from an alternatively spliced transcript of the calcitonin gene[26] and belongs to a superfamily of related peptides. CGRP is predominantly expressed in the central and peripheral nervous systems[27] and usually co-localized with substance P in sensory c-fiber afferents in the airway[28,29]. It has diverse biological effects that is mediated primarily through binding to and activating CGRP1 receptor. In earlier time, CGRP was described as a bronchi-constrictor for airways[30]. This effect, however, is discordant with its ability to activate adenylate cyclase which results in an increase in cyclic AMP level in cells, a pathway usually associated with bronchi-dilatation[31]. Other studies performed in isolated guinea pig or human airways have not shown CGRP having any bronchi-constriction effects, instead, it attenuated reaction to methacholine in allergic mouse[32]. To explain these contradictory data, it is necessary to explore further the role of CGRP in lung injury. Our results have shown that, in different stages of lung injury, the level of CGRP in lung changed in a similar

way as VIP, but peaked somewhat earlier than VIP. In earlier period, concentration of CGRP increased within 24 h and peaked on d 2, then decreased gradually. When lung injury aggravated due to the continued ozone exposure, the level of CGRP surprisingly began to go down, which clued that CGRP wasn't the direct factor causing lung injury. Earlier studies in our laboratory have proved that CGRP can upregulate ICAM-1 expression in BECs while the cells are in a stressed condition, and induce polymorphnuclear leukocytes and eosinophils to infiltrate into lung[33]. It has been reported that CGRP has a potent and long-lasting vasodilating effect[34]. Unlike substance P, CGRP doesn't induce mucus hypersecretion or plasma extra-exudation in the airways[35]. Therefore our study supports that CGRP exerts an earlier role in modulating airway function including triggering inflammatory reaction, helping to eliminate allergens and to cease lung injury by stimulating BECs to release cytokines and express ICAM-1.

For understanding clearly the role of intrapulmonary neuropeptide in the development of AHR, it is necessary to investigate expression and time-space contribution of neuropeptide receptor in lung. In our experiments, determination of mRNA encoding neuropeptide receptors demonstrated time-dependent increases in VIPR1 and CGRPR1 in lung. Increase of VIPR1 mRNA was detectable at 2 d, being maximal at 2 to 4 d, and then decreased gradually. Increase in CGRPR1 was at maximum at 4 d and the peak value of VIPR1 lasted longer than that of CGRPR1. These data indicate that both VIP receptor and CGRP receptor are expressed at high density in lung during the injury compensatory period, which is benefit for inhibiting a possible over-extensive inflammatory response. However, in the decompensation period, they decrease due to the loss of cell function. The time course of expression change of the two receptors paralleled with the increases in VIP and CGRP in lung. In our study, *in situ* hybridization for neuropeptide receptors demonstrated that, from d 2 to 4, VIPR1 and CGRPR1 positive cells appeared around vessels and small bronchus, and on d 8, very few positive cells were seen in lung, which appeared concurrently with the increase in concentration of neuropeptides in lung tissue. Our kinetic data imply that CGRP and VIP may exert sequential protective effects on AHR.

We conclude from the results of this study that intrapulmonary neuropeptides VIP and CGRP play important roles in the development of AHR, which will provide new insight into the prevention and clinical treatment of airway diseases.

ACKNOWLEGEMENTS: We thank Prof. WEN Ji-Fang (Department of Pathology, XiangYa Medical College, Central South University) for his help in histopathologic examination.

REFERENCE

1 Ward C, Pais M, Bish R, Reid D, Feltis B, Johns D, Walters EH. Airway inflammation, basement membrane thickening and bronchial hyperresponsiveness in asthma. Thorax 2002;57(4): 309-316.

2 Laprise C, Laviolette M, Boutet M, Boulet LP. Asymptomatic airway hyperresponsiveness: relationships with airway inflammation and remodelling. Eur Respir J 1999;14(1):63-73.

3 Ingenito EP, Ingram RH Jr. Early and late-phase bronchoconstriction after allergen challenge of nonanesthetized guinea pigs. Am Rev Respir Dis 1989;139(2):569.

4 Chan-Yeung M, Malo JL. Aetiological agents in occupational asthma. Eur Respir J 1994;7(2):346-371.

5 Watanabe A, Hayashi H. Allergen-induced biphasic bronchoconstriction in rats, Int Arch Allergy Appl Immunol 1990; 93(1): 26-34.

6 Folkerts G, Nijkamp FP. Airway epithelium: more than just a barrier. Trends Pharmacol Sci 1998;19(8):334-341.

7 Qin XQ (秦晓群), Xiang Y, Luo ZQ, Zhang CQ, Sun XH. Fibronectin or RGD peptide promotes nitric oxide synthesis of rabbit bronchial epithelial cells. Acta Physiol Sin (生理学报) 2000;52(6):519-521 (Chinese, English abstract).

8 Maggi CA, Giachetti A, Dey RD, Said SI. Neuropeptides as regulators of airway function: vasoactive intestinal peptide and the tachykinins. Physiol Rev 1995;75(2):277-322.

9 Martling CR. Sensory nerves containing tachykinins and CGRP in the lower airways. Functional implications for bronchoconstriction, vasodilatation and protein extravasation. Acta Physiol Scand Suppl 1987;563:1-57.

10 Qin XQ (秦晓群), Sun XH, Zhang CQ. Cytoprotective effects of vasoactive intestinal peptide on rabbit bronchial epithelial cells damaged by ozone exposure. Chin J Appl Physiol (中国应用生理学杂志) 1998;14:250-253 (Chinese, English abstract).

11 Tan YR (谭宇蓉), Qin XQ, Guan CX, Zhang CQ, Xiang Y, Ren YH. Influence of regulatory peptides on the secretion of interleukins from bronchial epithelial cells of the rabbit. Acta Phydiol Sin (生理学报) 2002;54(2):107-110 (Chinese, English abstract).

12 Tan YR (谭宇蓉), Qin XQ, Guan CX, Zhang CQ. Effects of regulatory peptides on adhesion of eosinophil to bronchial epithelial cells. Acta Physiol Sin (生理学报) 2002;54(1):43-46 (Chinese, English abstract).

13 Holgate ST. Epithelial damage and response. Clin Exp Allergy 2000;30 (Suppl 1):37-41.

14 Piedimonte G. Tachykinin peptides, receptors, and peptidases in airway disease. Exp Lung Res 1995;21(6):809-834

15 Barnes PJ, Baraniuk JN, Belvisi MG. Neuropeptides in the respiratory tract. Part II. Am Rev Respir Dis. 1991;144(6):1391-1399.

16 Casale TB. Neuropeptides and the lung. J Allergy Clin Immunol 1991;88(1):1-14.

17 Barnes PJ. Neurogenic inflammation in the airways. Respir Physiol 2001;125(1-2):145-154.

18 Dey RD, Shannon WA Jr, Said SI. Localization of VIP-immunoreactive nerves in airways and pulmonary vessels of dogs, cats, and human subjects. Cell Tissue Res 1981;220(2): 231-238.

19 Lundberg JM, Fahrenkrug J, Hokfelt T, Martling CR, Larsson O, Tatemoto K, Anggard A. Co-existence of peptide HI (PHI) and VIP in nerves regulating blood flow and bronchial smooth muscle tone in various mammals including man. Peptides 1984;5(3):593-606.

20 Carstairs JR, Barnes PJ. Visualization of vasoactive intestinal peptide receptors in human and guinea pig lung. J Pharmacol Exp Ther 1986;239(1):249-255.

21 Said SI, Dickman KG. Pathways of inflammation and cell death in the lung: modulation by vasoactive intestinal peptide. Regul Pept 2000;93(1-3):21-29.

22 Said SI. The Viktor Mutt Memorial Lecture. Protection by VIP and related peptides against cell death and tissue injury. Ann N Y Acad Sci 2000;921:264-274.

23 Morice A, Unwin RJ, Sever PS. Vasoactive intestinal peptide causes bronchodilatation and protects against histamine-induced bronchoconstriction in asthmatic subjects. Lancet 1983;2(8361): 1225-1227.

24 Kaltreider HB, Ichikawa S, Byrd PK, Ingram DA, Kishiyama JL, Sreedharan SP, Warnock ML, Beck JM, Goetzl EJ. Upregulation of neuropeptides and neuropeptide receptors in a murine model of immune inflammation in lung parenchyma. Am J Respir Cell Mol Biol 1997;16(2):133-144.

25 Lilly CM, Kobzik L, Hall AE, Drazen JM. Effects of chronic airway inflammation on the activity and enzymatic inactivation of neuropeptides in guinea pig lungs. J Clin Invest 1994;93(6): 2667-2674.

26 Amara SG, Jonas V, Rosenfeld MG, Ong ES, Evans RM. Alternative RNA processing in calcitonin gene expression generates mRNAs encoding different polypeptide products. Nature 1982;298(5871):240-244.

27 Poyner DR. Calcitonin gene-related peptide: multiple actions, multiple receptors. Pharmacol Ther 1992;56(1):23-51.

28 Lundberg JM, Franco-Cereceda A, Hua X, Hokfelt T, Fischer JA. Co-existence of substance P and calcitonin gene-related peptide-like immunoreactivities in sensory nerves in relation to cardiovascular and bronchoconstrictor effects of capsaicin. Eur J Pharmacol 1985;108(3):315-319.

29 Martling CR. Sensory nerves containing tachykinins and CGRP in the lower airways. Functional implications for bronchoconstriction, vasodilatation and protein extravasation. Acta Physiol Scand Suppl 1987;563:1-57.

30 Palmer JB, Cuss FM, Mulderry PK, Ghatei MA, Springall DR, Cadieux A, Bloom SR, Polak JM, Barnes PJ. Calcitonin gene-related peptide is localised to human airway nerves and potently constricts human airway smooth muscle. Br J Pharmacol 1987;91(1):95-101.

31 Sigrist S, Franco-Cereceda A, Muff R, Henke H, Lundberg JM, Fischer JA. Specific receptor and cardiovascular effects of calcitonin gene-related peptide. Endocrinology 1986;119(1): 381-389.

32 Dakhama A, Kanehiro A, Makela MJ, Loader JE, Larsen GL, Gelfand EW. Regulation of airway hyperresponsiveness by calcitonin gene-related peptide in allergen sensitized and challenged mice. Am J Respir Crit Care Med 2002;165(8):1137-1144.

33 Tan YR, Qin XQ, Guan CX, Zhang CQ, Luo ZQ. Regulatory peptides modulate ICAM-1 gene expression and NF-κB activity in bronchial epithelial cells. Acta Physiol Sin 2003; 55(2):121-127.

34 Brain SD, Williams TJ, Tippins JR, Morris HR, MacIntyre I. Calcitonin gene-related peptide is a potent vasodilator. Nature 1985;313(5997):54-56.

35 Webber SE, Lim JC, Widdicombe JG. The effects of calcitonin gene-related peptide on submucosal gland secretion and epithelial albumin transport in the ferret trachea *in vitro*. Br J Pharmacol 1991;102(1):79-84.